Mixing behavior of identical molecular weight phosphatidylcholines with various chain-length differences in two-component lamellae

Robert B. Sisk, Zhao-qing Wang, Hai-nan Lin, and Ching-hsien Huang
Department of Biochemistry, Health Sciences Center, University of Virginia, Charlottesville, Virginia 22908 USA

ABSTRACT It has recently been suggested that mixed-chain phosphatidylcholines with normalized chain length differences ($\Delta C/CL$) in the range of 0.10–0.40 undergo spontaneous self-assembly in excess water at $T < T_m$ into the partially interdigitated bilayer and those with $\Delta C/CL$ values in the range of 0.44–0.57 form, in excess water, mixed interdigitated bilayers at $T < T_m$. The mixing behavior of binary mixtures of C(22):C(12)PC/C(17):C(17)PC, C(22):C(12)/C(15):C(19)PC, and C(15):C(19)PC/C(13):C(21)PC reported in this work is used to support this view. The values of $\Delta C/CL$ for C(17):C(17)PC, C(15):C(19)PC, C(13):C(21)PC, and C(22):C(12)PC are 0.10, 0.15, 0.35, and 0.55, respectively. The binary mixture of C(15):C(19)PC/C(13):C(21)PC exhibits a lens-shaped phase diagram, indicating that these two identical molecular weight (MW) lipids with $\Delta C/CL$ values <0.4 are completely miscible over the entire compositional range in both gel and liquid-crystalline phases. In contrast, the phase diagrams of C(22):C(12)PC/C(17):C(17)PC and C(22):C(12)PC/C(15):C(19)PC are eutectic, indicating immiscibility of the component lipids over a wide compositional range in the gel phase. This immiscibility of identical MW lipids in the bilayer plane can be attributed to the different packing properties of the component lipids in the bilayer at $T < T_m$.

INTRODUCTION

The static and dynamic conformation of the two acyl chains in a phosphatidylcholine molecule are known to be inequivalent in bilayers and biological membranes (Yeagle, 1987). Specifically, the initial segment of the *sn*-2 acyl chain runs parallel to the bilayer surface and then bends over at the bond between carbon 2 and 3 so that the rest of the *sn*-2 acyl chain runs parallel to the *sn*-1 acyl chain. Because of the sharp bend on the *sn*-2 acyl chain, the two acyl chains are different in their chain lengths, being separated along the long molecular axis by 1.5 carbon–carbon bond lengths for identical-chain phosphatidylcholine in the gel-state bilayer (Zaccai et al., 1979). The normalized chain-length difference between the *sn*-1 and *sn*-2 acyl chains for a phosphatidylcholine molecule in the gel-state bilayer can be quantitatively expressed as $\Delta C/CL$, where ΔC is the effective chain-length difference, in C–C bonds, between the two acyl chains, and CL is the effective length of the longer of the two acyl chains, in C–C bonds. In calculating the value of ΔC and CL, an inherent shortening of 1.5 C–C bond lengths for the *sn*-2 acyl chain must be taken into account; for instance, the value of ΔC can be calculated from the relationship: $\Delta C = |n_1 - n_2 + 1.5|$, where n_1 and n_2 are the number of carbon atoms in the *sn*-1 and *sn*-2 acyl chains, respectively (Mason et al., 1981).

The effect of chain-length difference between the *sn*-1 and *sn*-2 acyl chains in lipid molecules on the thermotropic phase behavior of the lipid bilayer has been studied recently by high-resolution differential scanning calorimetry (DSC)[1] using a series of mixed-chain phosphatidylcholines with a common molecular weight (MW) which is identical to that of C(17):C(17)PC (Huang, 1990; Lin et al., 1990). Results from these DSC studies demonstrate that the thermodynamic parameters (T_m, ΔH, and ΔS) associated with the main phase transition for dispersions of C(17):C(17)PC, C(15):C(19)PC, C(18):C(16)PC, C(14):C(20)PC, C(19):C(15)PC, C(13):C(21)PC, and C(20):C(14)PC are inversely related to the corresponding values of the normalized chain-length difference ($\Delta C/CL$) for these lipids. The values of $\Delta C/CL$ for these seven species of phosphatidylcholines are within the range of 0.1 to 0.4. This linear relationship suggests that these fully hydrated mixed-chain phosphatidylcholines and C(17):C(17)PC are packed similarly in the bilayer at $T < T_m$; in addition, the negative slope suggests that the conformational statistics of the hydrocarbon chain and hence the lateral chain–chain interactions of these mixed-chain phosphatidylcholines in the gel-state bilayer are perturbed proportionally by a progressive increase in the

Address reprint requests to Dr. Ching-hsien Huang.

[1] *Abbreviations used in this paper:* C(*X*):C(*Y*)PC, saturated L-α-phosphatidylcholine having *X* carbons in the *sn*-1 acyl chain and *Y* carbons in the *sn*-2 acyl chain; DSC, differential scanning calorimetry; MW, molecular weight; T_m, main phase transition temperature.

0006-3495/90/09/777/07 $2.00

normalized chain-length difference. The physical basis for the perturbation may be attributed to the bulky methyl termini of the lipid acyl chains. Because the effective volume of the chain terminal methyl group is about twice that of a methylene group in the hydrocarbon chain (Reiss-Husson and Luzzati, 1964; Nagle and Wiener, 1988), it can be expected that the bulky methyl ends will distort the all-*trans* conformation of the nearby methylene groups in a closely packed gel-state bilayer. In addition, this terminal distortion tends to propagate itself along the rest of the acyl chain in the gel-state bilayer as the two terminal methyl groups within the same lipid molecule are progressively displaced further away from each other. Consequently, the conformational statistics of the acyl chain and the lateral chain–chain van der Waals contact interactions in the gel-state bilayer are perturbed progressively by increasing the values of $\Delta C/CL$.

When the value of $\Delta C/CL$ for the various identical MW phosphatidylcholines reaches the range of 0.42–0.57, the DSC results show that the thermodynamic parameters associated with the main phase transition deviate markedly from the linear function observed in the T_m (ΔH or ΔS) vs. $\Delta C/CL$ plot for those less asymmetric lipids with $\Delta C/CL = 0.1$–0.4. Presumably, this deviation is caused by a different mode of chain packing for these highly asymmetric phosphatidylcholines in the gel-state bilayer. Specifically, we suggest that phosphatidylcholines with $\Delta C/CL = 0.1$–0.4 undergo spontaneous self assembly in excess water into a partially interdigitated bilayer at $T < T_m$, in which the longer chain of the lipid on one side of the bilayer packs end-to-end with the shorter chain of another lipid molecule in the opposing bilayer leaflet. When the value of $\Delta C/CL$ is greater than 0.40, the chain-end perturbation becomes so overwhelming that these highly asymmetric lipid molecules can no longer self-assemble into the partially interdigitated bilayer at $T < T_m$; they have to assume a new equilibrium packing in the gel-state bilayer, leading to a mixed interdigitated packing mode. In this new packing mode, the long acyl chain spans the whole width of the bilayer's hydrocarbon core and the short chains, each from a lipid molecule in the opposing leaflet, meet end-to-end in the bilayer midplane. This packing mode, called the mixed interdigitated bilayer, has been detected by x-ray diffraction techniques for fully hydrated C(18):C(10)PC at $T < T_m$ (McIntosh et al., 1984; Hui et al., 1984; Mattai et al., 1987), and the value of $\Delta C/CL$ for C(18):C(10)PC is 0.56. In fact, based on thermodynamic data, it has been inferred that the mixed interdigitated packing mode observed for C(18):C(10)PC bilayers at $T < T_m$ can be applied to all fully hydrated mixed-chain phosphatidylcholines with values of $\Delta C/CL$ in the range of 0.44–0.57 (Xu and Huang, 1987; Huang, 1990). In this packing mode, the terminal methyl group of the long acyl chain is intercalated into the bilayer interface and it is positioned in the vicinity of the carbonyl carbon in the opposing leaflet. The lateral chain–chain packing constraint imposed by the chain terminal perturbation is thus greatly released in the mixed interdigitated bilayer, resulting in a more ordered lamellar structure for the gel-state bilayer of mixed-chain phosphatidylcholines. However, the bilayer thickness of the mixed interdigitated bilayer is considerably smaller than that of the partially interdigitated bilayer. The lipid species which have the same MW as that of C(17):C(17)PC with $\Delta C/CL$ values in the range of 0.44–0.57 are C(12):C(22)PC ($\Delta C/CL = 0.44$), C(21):C(13)PC ($\Delta C/CL = 0.48$), and C(22):C(12)PC ($\Delta C/CL = 0.55$).

If mixed-chain phosphatidylcholines with values of $\Delta C/CL$ in the range of 0.44–0.57 do self-assemble into the mixed interdigitated bilayer in excess water at $T < T_m$, one would expect *a priori* that these lipids would not mix ideally in the gel-state bilayer with those identical MW mixed-chain phosphatidylcholines having values of $\Delta C/CL$ in the range of 0.1–0.40 due to the large difference (~33%) in the bilayer thickness between the mixed interdigitated and partially interdigitated bilayers at $T < T_m$. In fact, one is most likely to detect extensive phase separation in the gel state for the binary mixture and to observe a eutectic phase diagram similar to the binary phase diagram of C(18):C(10)PC/C(14):C(14)PC (Lin and Huang, 1988).

In light of the above considerations, we have examined calorimetrically the mixing behavior of the following binary mixtures of identical MW phosphatidylcholines: C(17):C(17)PC($\Delta C/CL = 0.094$)/C(22):C(12)PC ($\Delta C/CL = 0.548$), C(15):C(19)PC ($\Delta C/CL = 0.152$)/C(22):C(12)PC, and C(15):C(19)PC/C(13):C(21)PC ($\Delta C/CL = 0.350$). The phase diagrams obtained with these binary mixtures indeed show that the miscibility and immiscibility between these pairs of identical MW phosphatidylcholines in the bilayer are consistent with the partially interdigitated and mixed interdigitated packing models proposed for the various lipid species with their characteristic values of $\Delta C/CL$. These mixed-chain phosphatidylcholines were prepared by acylation of appropriate lysophosphatidylcholines with desired fatty acid anhydrides at room temperature by using 4-pyrrolidinopyridine as catalyst as described elsewhere (Xu and Huang, 1987). The identical-chain phosphatidylcholine, C(17):C(17)PC, was purchased from Avanti Polar Lipids, Inc. (Birmingham, AL). Sample preparations and the thermal scan of the sample with a Microcal MC-2 microcalorimeter at a constant heating or cooling rate of 15°C/h were described in detail elsewhere (Lin and Huang, 1988; Lin et al., 1990). Before the initial DSC heating scan, all samples have been preincubated at 0°C for an extended period (>2 wk).

RESULTS AND DISCUSSION

Fig. 1 shows a series of DSC heating thermograms for binary mixtures of C(22):C(12)PC/C(15):C(19)PC dispersed in aqueous NaCl solution (50 mM) containing 5 mM phosphate buffer and 1 mM EDTA at pH 7.4. Within the compositional range of 0–45 mol% C(15):C(19)PC, the main phase transition temperature (T_m) of the transition curve decreases steadily from 43.1 to 36.0°C, and the decrease in T_m is accompanied first by a broadening of the transition curve up to 15 mol% C(15):C(19)PC and then by a narrowing of the curve upon further incorporating C(15):C(19)PC up to ~45 mol%. Between 50 and 100 mol% C(15):C(19)PC, a reverse trend is observed for the change in T_m which increases progressively from 36°C at 50 mol% to 45.0°C at 100 mol% C(15):C(19)PC. The up-shift in T_m values is accompanied first by a broadening and then by a narrowing of the transition curves. It should be noted that a prominent subtransition at 36.0°C is observed for the pure C(15):C(19)PC sample (Fig. 1). This subtransition has been reported previously (Lin et al., 1990), and it disappears on subsequent cooling. In fact, the subtransitions are discernible in binary mixtures of C(22):C(12)PC/C(15):C(19)PC containing 20 mol% or more of C(15):C(19)PC; however, they are irreversible on cooling and immediate reheating (data not shown).

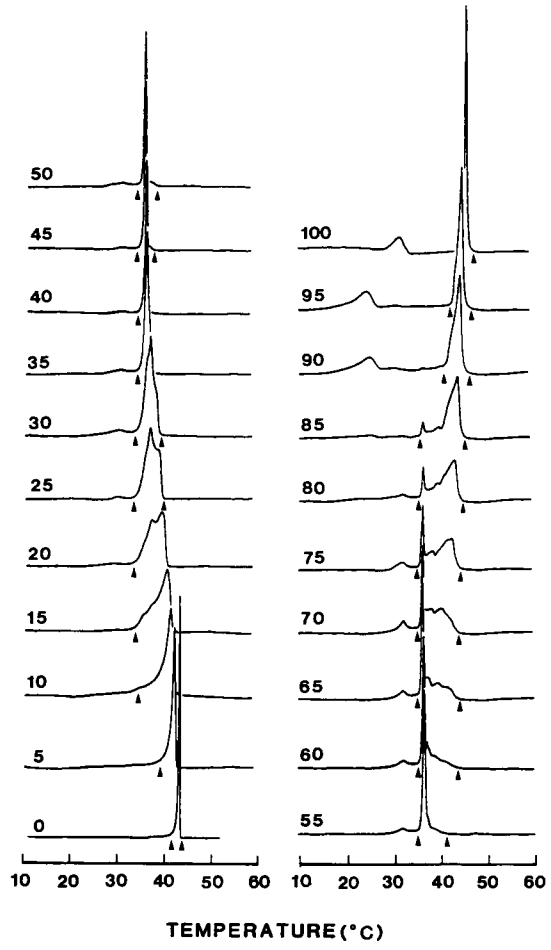

FIGURE 1 DSC heating thermograms for aqueous dispersions of C(22):C(12)PC containing various contents of C(15):C(19)PC. The mole percent of C(15):C(19)PC in each of the binary mixtures is indicated adjacent to respective thermograms. The onset and completion temperatures of the various main transitions are indicated by the triangles.

The temperature-composition phase diagram for binary mixtures of C(22):C(12)PC/C(15):C(19)PC derived from the various main transition curves shown in Fig. 1 is illustrated in Fig. 2 *A*. The values of the onset and completion temperatures of the main transitions as indicated by the triangles in Fig. 1 have been corrected by assuming a zero linewidth of the phase transition of the single pure component lipids (Mabrey and Sturtevant, 1976); these corrected onset and completion temperatures define the solidus and liquidus boundaries of the phase

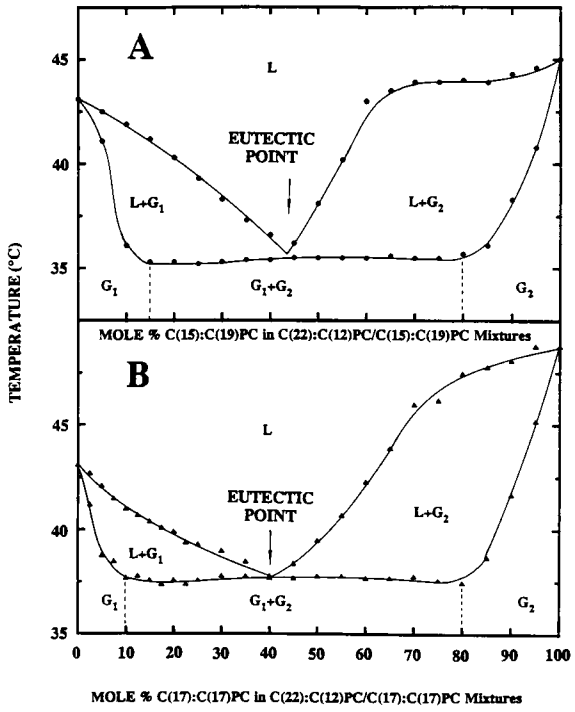

FIGURE 2 Temperature-composition phase diagrams for C(22):C(12)PC/C(15):C(19)PC (*A*) and C(22):C(12)PC/C(17):C(17)PC (*B*) mixtures. The lower and upper solid lines of the phase boundaries in each phase diagram are drawn by hand to fit the onset and completion temperatures, respectively, of the transition curves for the various mixtures after correction for the finite width of the transition curves of the pure components. The dotted vertical lines represent the solvus lines, corresponding approximately to the two ends of the eutectic horizontal.

diagram, respectively. The phase diagram shown in Fig. 2 *A* exhibits the characteristic shape indicative of a eutectic system for aqueous dispersions of C(22):C(12)PC/C(15):C(19)PC mixtures. Clearly, the eutectic point is at 35.5°C and 44 mol% of C(15):C(19)PC. It is important to note that the eutectic horizontal at 35.5°C covers a wide compositional range of 15–80 mol% C(15):C(19)PC, indicating an extensive phase separation of gel phases (G_1 and G_2) for the binary mixture at temperatures below the eutectic horizontal. Above the liquidus boundary, the two component lipids are totally miscible in the fluid bilayer, leading to a single liquid-crystalline (L_α) phase. Between the phase boundaries and separated by the eutectic point are two distinct two-phase regions in which the gel phase (G_1 or G_2) and the liquid-crystalline L_α phase are in thermodynamic equilibrium; however, the lipid molecules in the gel as well as the L_α phase are most likely aggregated into separate domains within the two-dimensional plane of the bilayer structure. The general conclusion from this eutectic phase diagram is that C(22):C(12)PC and C(15):C(19)PC tend to exhibit gel–gel phase immiscibility at temperatures below 35.5°C over a wide compositional range, whereas the binary mixtures are completely miscible when the component lipids are both in the liquid-crystalline phase.

To eliminate any possible shift in the position of the main phase transition as induced by the subtransition, the second and third DSC heating scans of C(22):C(12)PC/C(15):C(19)PC mixtures have also been recorded and analyzed. In these thermograms, no subtransitions are observed. The onset and completion temperatures of the various main phase transitions, after appropriate corrections, were used to construct the phase diagrams. Within the experimental error, the phase diagrams derived from the second and third DSC heating scans are virtually indistinguishable from the one shown in Fig. 2 *A*.

Fig. 3 shows the third DSC heating curves for a series of samples containing various amounts of C(17):C(17)PC in the C(22):C(12)PC/C(17):C(17)PC mixtures. As the mole percent of C(17):C(17)PC incorporated into C(22):C(12)PC is increased from 0 to 40, the single phase transition curve of C(22):C(12)PC at 43.1°C shifts progressively toward lower temperatures; in addition, the transition curve is first broadened gradually and then narrowed successively. At 40 mol% C(17):C(17)PC, the DSC heating thermogram displays a single symmetric transition curve peaked at 37.6°C. Above 40 mol% of C(17):C(17)PC, the peak position of the transition curve shifts continually towards higher temperatures until it reaches the maximal value of 49.0°C at 100 mol% C(17):C(17)PC. The transition curve broadens gradually and symmetrically from 40 to 50 mol% C(17):C(17)PC; at higher C(17):C(17)PC content up to ~80 mol%, the phase transition curve of the binary lipid mixture is

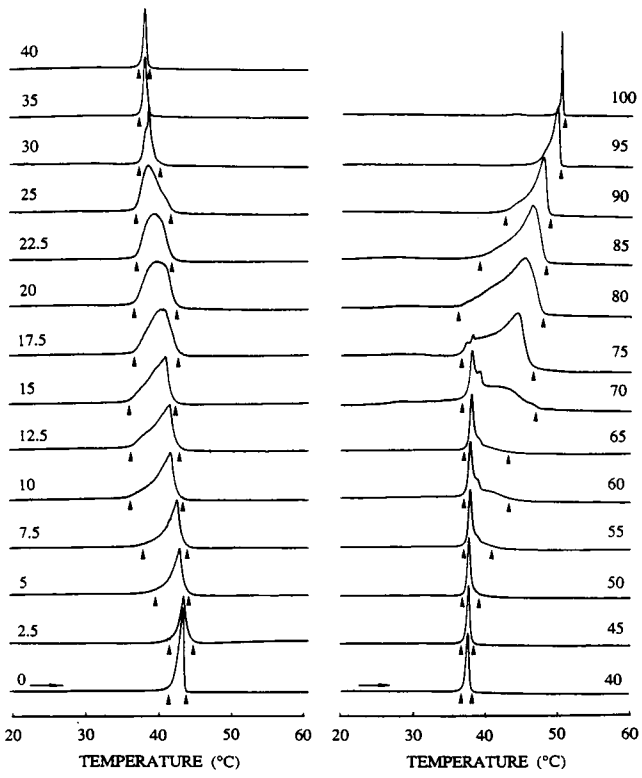

FIGURE 3 DSC heating thermograms for aqueous dispersions of C(22):C(12)PC containing various contents of C(17):C(17)PC. The curves are plotted stepwise in an increasing concentration of C(17):C(17)PC, in mole percent, as indicated adjacent to respective thermograms. The onset and completion temperatures of the various transitions are indicated by the triangles. Arrows indicate the direction of temperature change in the DSC scans.

characterized by asymmetric broadening and complex shape. However, above 80 mol% C(17):C(17)PC, the transition curve begins to narrow until the composition reaches 100 mol% C(17):C(17)PC. For the pure C(17):C(17)PC sample, a pretransition peaked at 42.7°C is discernible.

The temperature-composition phase diagram of C(22):C(12)PC/C(17):C(17)PC mixtures, constructed based on the onset and completion temperatures of the various transition curves as indicated by the triangles in Fig. 3, is shown in Fig. 2 *B*. The eutectic phase diagram, shown in Fig. 2 *B*, is similar to the one shown in Fig. 2 *A*. The eutectic point is observed at 37.5°C and 40 mol% C(17):C(17)PC and the eutectic horizontal at 37.5°C extends from 10 to 85 mol% of C(17):C(17)PC. Again, this phase diagram is, within the experimental error, virtually identical to the one derived from the first and second DSC heating scans of the same samples.

The observation of eutectic phase diagrams for both C(22):C(12)PC/C(17):C(17)PC and C(22):C(12)PC/

C(15):C(19)PC mixtures indicates the formation of separate gel domains of wide compositional ranges of C(22):C(12)PC and C(17):C(17)PC and of C(22):C(12)PC and C(15):C(19)PC. Furthermore, these phase diagrams also indicate that mixtures of these binary component lipids are miscible in the liquid-crystalline phase. The observed mixing behavior of these lipids in the plane of the bilayer in both the gel and liquid-crystalline phases is indeed consistent with the different packing models proposed for the component lipids. As discussed earlier, saturated phosphatidylcholines with $\Delta C/CL$ values in the range of 0.1–0.4 are proposed to form, at $T < T_m$, the partially interdigitated bilayer, whereas those with $\Delta C/CL$ values in the range of 0.44–0.57 are suggested to self-assemble in excess water into the mixed interdigitated bilayer at $T < T_m$. The values of $\Delta C/CL$ for C(17):C(17)PC, C(15):C(19)PC, and C(22):C(12)PC are 0.1, 0.15, and 0.55, respectively. Hence, C(17):C(17)PC and C(15):C(19)PC tend to form partially interdigitated bilayers at $T < T_m$, and C(22):C(12)PC having one acyl chain almost twice the length of the other undergoes spontaneous self-assembly, at $T < T_m$, into the mixed interdigitated bilayer in excess water. The wide range of immiscibility of C(22):C(12)PC/C(17):C(17)PC and C(22):C(12)PC/C(15):C(19)PC mixtures in the gel phase as shown in the eutectics can thus be attributed to the mismatch of the bilayer thickness between the partially interdigitated bilayer enriched with either C(17):C(17)PC or C(15):C(19)PC and the mixed interdigitate bilayer enriched with C(22):C(12)PC. At $T > T_m$, the mixed interdigitated bilayer converts into the partially interdigitated bilayer (McIntosh et al., 1984; Hui et al., 1984; Mattai et al., 1987). Consequently, each identical pair (A–A or B–B) of the component lipids in C(22):C(12)PC/C(17):C(17)PC or C(22):C(12)PC/C(15):C(19)PC mixtures at $T > T_m$ forms a packing unit across the lipid bilayer (Xu et al., 1987), and these packing units (A–A or B–B) are miscible laterally in the bilayer plane of the fluid bilayer due to their nearly identical packing characteristics at $T > T_m$.

Having demonstrated that binary mixtures of C(22):C(12)PC/C(17):C(17)PC and C(22):C(12)PC/C(15):C(19)PC form eutectics in the two-dimensional plane of the lipid bilayer, the mixing behavior of C(15):C(19)PC/C(13):C(21)PC mixtures was then investigated calorimetrically as a function of temperature. Because the values of $\Delta C/CL$ for C(15):C(19)PC and C(13):C(21)PC are 0.15 and 0.35, respectively, these lipids are expected to self-assemble in excess water into a similar packing model of partially interdigitated bilayers at $T < T_m$ (Huang, 1990; Lin et al., 1990). At temperatures above the T_m, the partially interdigitated bilayer converts to the liquid-crystalline L_α phase. Because the total number of methylene units in the two acyl chains of C(15):C(19)PC is the same as that of C(13):C(21)PC and because these two lipid species are presumably packed into a common mode of bilayer structures at temperatures both above and below the main phase transition temperature, the bilayer thickness of C(15):C(19)PC can thus be expected to be virtually identical to that of C(13):C(21)PC at all temperatures. Consequently, these two lipid species are expected to mix nearly ideally in all proportions in the two-dimensional bilayer plane in both gel and liquid-crystalline phases.

The initial heating thermogram for C(13):C(21)PC dispersions, illustrated in the bottommost DSC trace of Fig. 4 *A*, exhibits a single symmetric transition with $T_m = 34.0°C$ and $\Delta H = 18.7$ kcal/mol. This endothermic transition with an unusually high value of ΔH is assumed to correspond to the $L_c \rightarrow L_\alpha$ phase transition (Lin et al., 1990), where L_c is the crystalline phase and L_α is the fluid or liquid-crystalline phase. The cooling curve obtained immediately after the initial heating exhibits two distinct exotherms peaked at 33.7 and 16.1°C as shown in the bottommost DSC trace of Fig. 4 *B*. The high- and low-temperature exotherms appear to correspond to the $L_\alpha \rightarrow P_{\beta'}$ and $P_{\beta'} \rightarrow L_c$ phase transitions, respectively, where $P_{\beta'}$ is the rippled gel phase (Lin et al., 1990). The clear separation of the two exotherms allows the onset and completion temperatures of the main transition (or the $P_{\beta'} \leftrightarrow L_\alpha$ transition) to be determined unambiguously. Fig. 4 *A* also demonstrates that the progressive incorporation of C(15):C(19)PC into C(13):C(21)PC up to ~50 mol% results in a gradual splitting of the large endothermic transition of C(13):C(21)PC into two endothermic transitions, a low- and a high-temperature transitions. The distance between the two endothermic peaks increases with increasing mole fraction of C(15):C(19)PC. It is interesting to note that all the low-temperature transitions are abolished on subsequent cooling (Fig. 4 *B*); hence, they are subtransitions. In contrast, all the high-temperature transitions are reversible (Fig. 4 *B*), corresponding to the main phase transitions. It should perhaps be mentioned here that the prominent low-temperature transition exhibited by a prolonged preincubated sample of pure C(15):C(19)PC at 0°C, illustrated in the uppermost DSC trace of Fig. 4 *A*, has already been observed in Fig. 1 as displayed by a similarly preincubated sample of 100 mol% C(15):C(19)PC. This low-temperature transition peaked at ~31°C as detected in the first DSC heating scan is assigned as the subtransition of C(15):C(19)PC, because it disappears on subsequent cooling as demonstrated in the uppermost DSC trace of Fig. 4 *B*. In fact, this subtransition begins to appear in binary mixtures of C(15):C(19)PC/C(13):C(21)PC when the C(15):C(19)PC content reaches 80 mol% (Fig. 4 *A*).

The main phase transition temperature, T_m, of pure

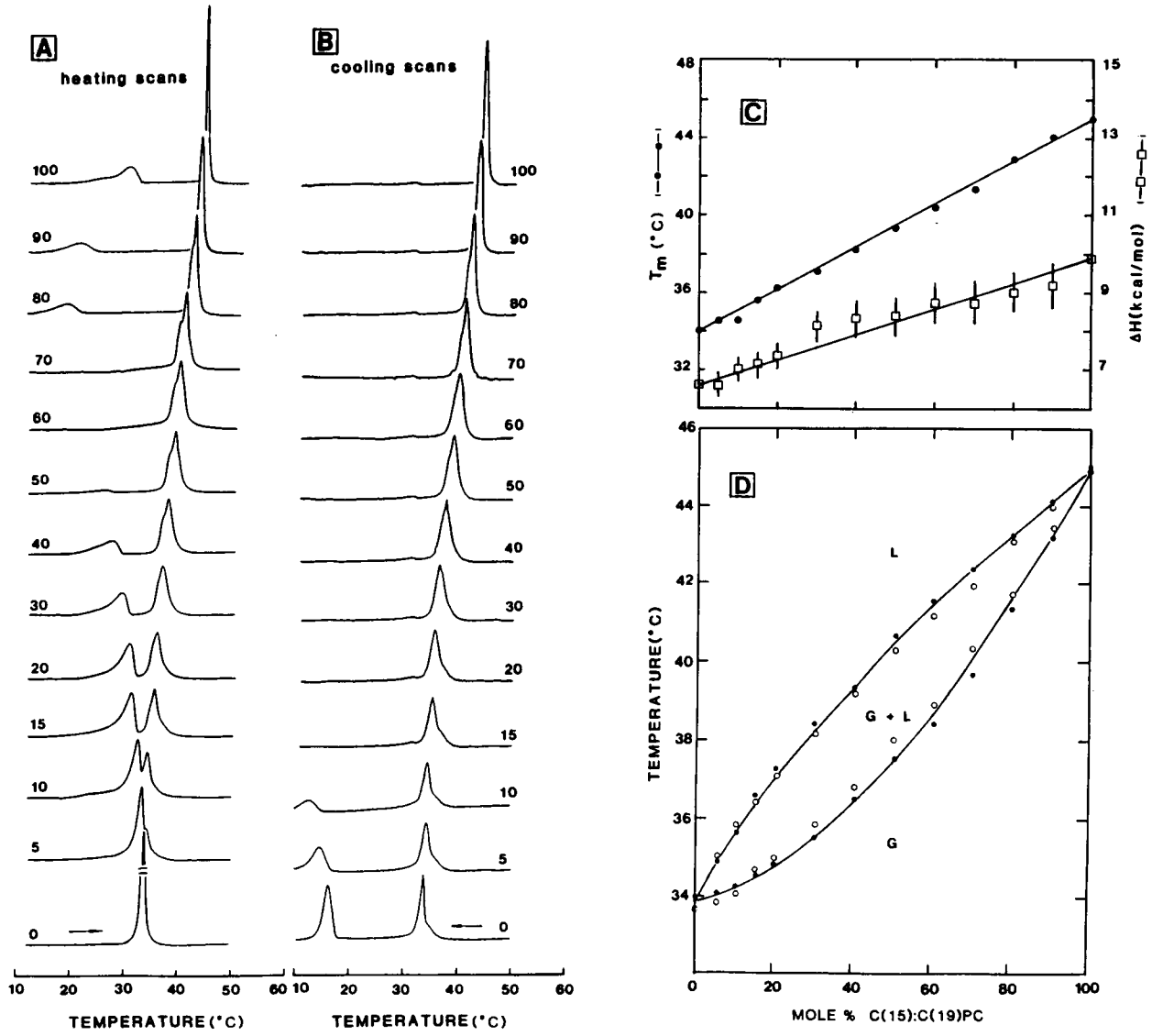

FIGURE 4 Thermal behavior of C(13):C(21)PC/C(15):C(19)PC mixtures. (*A*) Initial DSC heating scans of aqueous dispersions of C(13):C(21)PC/C(15):C(19)PC mixtures containing various C(15):C(19)PC contents as indicated in mole percent adjacent to respective scans. (*B*) The DSC cooling scans obtained immediately after *A*. Arrows in *A* and *B* show the direction of temperature change. (*C*) Dependence of T_m (*solid circles*) and ΔH (*open squares*) of the main phase transitions on the mole percent of C(15):C(19)PC in binary mixtures of C(13):C(21)PC/C(15):C(19)PC. (*D*) Temperature-composition phase diagram for the C(13):C(21)PC/C(15):C(19)PC system. The experimental data for the phase boundaries were determined, after correction for the finite width of the main phase transitions of the pure components, from the onset and completion temperatures of the main transitions derived from the heating (*solid circles*) and cooling (*open circles*) DSC curves shown in *A* and *B*, respectively. The solid lines are drawn by hand to fit the data of the onset and completion temperatures. *G* and *L* denote the gel and liquid-crystalline phases, respectively.

C(13):C(21)PC at 34.0°C is seen to increase linearly as the C(15):C(19)PC content is increased progressively (Fig. 4, *A* and *B*). In fact, the value of T_m for any of the binary mixtures is, within the experimental error, a mole fraction–weighted average of the corresponding T_m values for the pure components as shown in Fig. 4 *C*. Furthermore, addition of C(15):C(19)PC into the C(13):C(21)PC lamella results in increased ΔH with the increase being an essentially linear function of C(15):C(19)PC content (Fig. 4 *C*). Taken together, the data shown in Fig. 4 *C* indicate that C(13):C(21)PC and C(15):C(19)PC mix nearly ideally over the entire compositional range; hence, the expectation discussed earlier is indeed borne out by the experimental results. Moreover, the equilibrium phase diagram, derived from the main transitions shown in Fig. 4, *A* and *B*, after correction for the finite widths of the transitions of pure components, exhibits a lens shape (Fig. 4 *D*), reflecting the complete

miscibility of the two-component lipids with nearly ideal mixing in both gel and liquid-crystalline phases over the entire compositional range (Brumbaugh et al., 1990). This result is an excellent confirmation of our expectation that binary C(13):C(21)PC/C(15):C(19)PC mixtures should mix nearly ideally in the two-dimensional plane of the lipid bilayer based on the proposal that mixed-chain phosphatidylcholines with identical MW and with values of $\Delta C/CL = 0.1–0.4$ are packed into a partially interdigitated bilayer, at $T < T_m$, with nearly identical bilayer thickness.

In summary, the equilibria between two-component lipid mixtures of C(22):C(12)PC/C(17):C(17)PC, C(22):C(12)PC/C(15):C(19)PC, and C(15):C(19)PC/C(13):C(21)PC in the two-dimensional bilayer plane at various temperatures have been examined by high-resolution DSC, and the results are presented in this communication in terms of the phase diagram. The binary mixtures of C(22):C(12)PC/C(17):C(17)PC and C(22):C(12)PC/C(15):C(19)PC display eutectic phase diagrams (Fig. 2) indicative of gel phase immiscibility of the component lipids over a wide compositional range. In contrast, the phase diagram of C(15):C(19)PC/C(13):C(21)PC mixtures displays the characteristic lens shape (Fig. 4 *D*) indicative of nearly ideal mixing of the component lipids in both gel and liquid-crystalline phases. The observed phase diagrams are thus consistent with the proposal that phosphatidylcholines with values of $\Delta C/CL = 0.1–0.4$ are packed into the partially interdigitated gel-state bilayer at $T < T_m$, while those with values of $\Delta C/CL = 0.44–0.57$ are packed into the mixed interdigitated bilayer at $T < T_m$. The values of $\Delta C/CL$ for C(22):C(12)PC, C(13):C(21)PC, C(15):C(19)PC, and C(17):C(17)PC are 0.55, 0.35, 0.15, and 0.10, respectively.

This investigation was supported in part by National Institutes of Health grant GM-17452 from United States Public Health Service, Department of Health and Human Services, and by Instrumentation grant DiR-8907318 from the National Science Foundation.

Received for publication 18 April 1990 and in final form 1 June 1990.

REFERENCES

Brumbaugh, E. E., M. L. Johnson, and C. Huang. 1990. Non-linear least squares analysis of phase diagrams for non-ideal binary mixtures of phospholipids. *Chem. Phys. Lipids.* 53:69–78.

Huang, C. 1990. Mixed-chain phospholipids and interdigitated bilayer systems. *Klin. Wochenschr.* 68:149–165.

Hui, S. W., J. T. Mason, and C. Huang. 1984. Acyl chain interdigitation in saturated mixed-chain phosphatidylcholine bilayer dispersions. *Biochemistry.* 23:5570–5577.

Lin, H-n., and C. Huang. 1988. Eutectic phase behavior of 1-stearoyl-2-caprylphosphatidylcholine and dimyristoylphosphatidylcholine mixtures. *Biochim. Biophys. Acta.* 496:178–184.

Lin, H-n., Z-q. Wang, and C. Huang. 1990. A differential scanning calorimetry study of mixed-chain phosphatidylcholines with a common molecular weight identical to diheptadecanoyl phosphatidylcholine. *Biochemistry. 29:*7063–7072.

Mabrey, S., and J. M. Sturtevant. 1976. Investigation of phase transitions of lipids and lipid mixtures by high sensitivity differential scanning calorimetry. *Proc. Natl. Acad. Sci. USA.* 73:3862–3866.

Mason, J. T., C. Huang, and R. L. Biltonen. 1981. Calorimetric investigations of saturated mixed-chain phosphatidylcholine bilayer dispersions. *Biochemistry.* 20:6086–6092.

Mattai, J., P. K. Scripada, and G. G. Shipley. 1987. Mixed-chain phosphatidylcholine bilayer: structure and properties. *Biochemistry.* 26:3287–3297.

McIntosh, T. J., S. A. Simon, J. C. Ellington, and N. A. Porter. 1984. New structural model for mixed-chain phosphatidylcholine bilayers. *Biochemistry.* 23:4038–4044.

Nagle, J. F., and M. C. Wiener. 1988. Structure of fully hydrated bilayer dispersions. *Biochim. Biophys. Acta.* 942:1–10.

Reiss-Husson, F., and V. Luzzati. 1964. The structure of the micellar solutions of some amphiphilic compounds in pure water as determined by absolute small-angle x-ray scattering techniques. *J. Phys. Chem.* 68:3504–3511.

Xu, H., and C. Huang. 1987. Scanning calorimetric study of fully hydrated asymmetric phosphatidylcholines with one acyl chain twice as long as the other. *Biochemistry.* 26:1036–1043.

Yeagle, P. 1987. The Membranes of Cells. Academic Press, Inc., New York. Chapters 2 and 3.

Zaccai, G., G. Büldt, A. Seelig, and J. Seelig. 1979. Neutron diffraction studies on phosphatidylcholine model membranes. II. Chain conformation and segmental disorder. *J. Mol. Biol.* 134:693–706.